

## Note

Crystal and molecular structure of octakis(6-bromo-6-deoxy)- $\gamma$ -cyclodextrin. A novel stacking of a distorted macrocycleAnastasia Paulidou, Petros Giastas, Nikolaos Mourtzis,  
Konstantina Yannakopoulou and Irene M. Mavridis\**Institute of Physical Chemistry, National Center for Scientific Research 'Demokritos', Aghia Paraskevi 15310,  
PO Box 60228, Athens, Greece*Received 6 February 2007; received in revised form 10 May 2007; accepted 11 May 2007  
Available online 18 May 2007

**Abstract**—Octakis(6-bromo-6-deoxy)cyclomaltooctaose, perbrominated  $\gamma$ -cyclodextrin at the primary side, crystallises from methanol in a very unique manner. The macrocycles are quite distorted in contrast to their  $\beta$ -cyclodextrin analogue, heptakis(6-bromo-6-deoxy)cyclomaltoheptaose. The two monomers, arranged head-to-head, form a completely new kind of dimer by mutually entering into each other, both at the primary and the secondary sides. At the primary, hydrophobic side, they interact by  $\text{Br} \cdots \text{Br}$  interactions and at the secondary, hydrophilic side, by direct H-bonds between hydroxylic groups. The short contacts of the Br atoms contribute to the macrocycle's distortion, which is considerable compared to the few available structures of  $\gamma$ -CDs persubstituted at the primary side with bulkier and in some occasions charged substituents. Water and methanol molecules are entrapped in the cyclodextrin cavity, mostly in the area of the secondary hydroxylic groups connecting the macrocycles by indirect H-bonds. Thus the solvent molecules strengthen the association of the two monomers and contribute to the stabilisation of the cavity. The monomers stack along the  $a$ -axis and form columns that align in parallel lines along the same axis resulting in the formation of alternating hydrophobic and hydrophilic layers perpendicular to the  $a$ -axis resembling in this respect, the structure of the analogous perbrominated  $\beta$ -cyclodextrin.

© 2007 Elsevier Ltd. All rights reserved.

**Keywords:** Octakis(6-bromo-6-deoxy)- $\gamma$ -cyclodextrin; Per-6-brominated  $\gamma$ -cyclodextrin; Molecular structure; Amphiphilic  $\gamma$ -cyclodextrin

Modified cyclodextrins (CDs) are host molecules that can combine the properties of the attached functional groups and the inclusion characteristics of the macrocycle. Thus they can be used for applications ranging from functionalisation of surfaces to transfer of molecules through cell membranes. Due to the presence of numerous hydroxyl groups on the CD molecule, the modification of the latter presents many challenges, synthetic strategies depending on the desired product and its use. Primary hydroxyl groups can be modified easier than the secondary groups. However, persubstitution of the primary side is generally associated with steric hindrance effects that in turn may influence the geometry of the macrocycle, as well as induce rotational isomerism at the methylene carbon atoms. Nevertheless, the

chemistry of cyclodextrins has advanced considerably to provide a variety of *per*-substituted derivatives on the primary side of cyclodextrins.<sup>1</sup> Per-halogenation at the primary side<sup>2,3</sup> provides intermediates, such as heptakis(6-bromo-6-deoxy)cyclomaltoheptaose ( $\beta\text{pBr}$ )<sup>4</sup> and octakis(6-bromo-6-deoxy)cyclomaltooctaose ( $\gamma\text{pBr}$ ).<sup>5</sup>

Crystal structures of *per*-6-substituted CDs, as opposed to *per*-2,3,6-substituted CDs, are few. Only one modified  $\beta\text{CD}$ ,  $\beta\text{pBr}$ ,<sup>6</sup> and three modified  $\gamma\text{CDs}$  have been reported so far,<sup>7,8</sup> along with the complexes of two of them with the neuromuscular blocker, rocuronium bromide.<sup>8,9</sup> The latter  $\gamma\text{CD}$  structures present novel packing arrangements, probably dictated by their many functional groups, and various degrees of deformation of the macrocyclic backbone. More structures are welcome since the large size of  $\gamma\text{CD}$  seems to impose interesting features as it is quite flexible.

\* Corresponding author. E-mail: [mavridi@chem.demokritos.gr](mailto:mavridi@chem.demokritos.gr)

Presently, we report the structure of per-6-brominated  $\gamma$ CD,  $\gamma$ pBr, which exhibits interesting intermolecular interactions due to its amphiphilic character, as well as the flexibility of the  $\gamma$ CD torus.

**Molecular structure:** two crystallographically independent  $\gamma$ pBr hosts (A and B) comprise the asymmetric unit. The numbering scheme is given in Figure 1;<sup>10</sup> C(A or B)*mn* and O(A or B) *mn* denote the *m*th atom within the *n*th glucosidic residue (G*n*) of molecules A and B. Due to the distortion of the  $\gamma$ pBr monomers, the dimer geometry is unusual, because the macrocycles are not held together by the usual eight H-bonds between the secondary hydroxyl groups,<sup>11,12</sup> in contrast to  $\beta$ pBr, which in the crystalline state forms proper undistorted dimers.

The distorted molecules A and B are stacked head-to-head along the *a*-axis, offset from each other. As shown in Figure 2, the two monomers mutually enter into each other (Br atoms at the right side of A entering the primary side of B and vice versa) and form short intermolecular contacts that ensure cohesion along the *a*-axis. The secondary side association of the monomers is not very clear at this view angle. However, if seen rotated by 90° (Fig. 3), the macrocycle's secondary sides are related in a similar fashion as the primary (one side entering into the other) and they are tightly bound as discussed below.

The glucose residues have adopted the regular <sup>4</sup>C<sub>1</sub> chair conformation, as indicated by the puckering amplitude (*Q*) and  $\theta$  values calculated for the individual glucose residues.<sup>14</sup> *Q* values, in the range 0.608–0.489 Å for molecule A and 0.603–0.501 Å for B, respectively (Table 1), are close to the values of the ideal cyclohexane chair (*Q* = 0.63 Å). Similarly, the small  $\theta$  values, 2.22°–8.12° for molecule A and 2.76°–10.34° for mol-

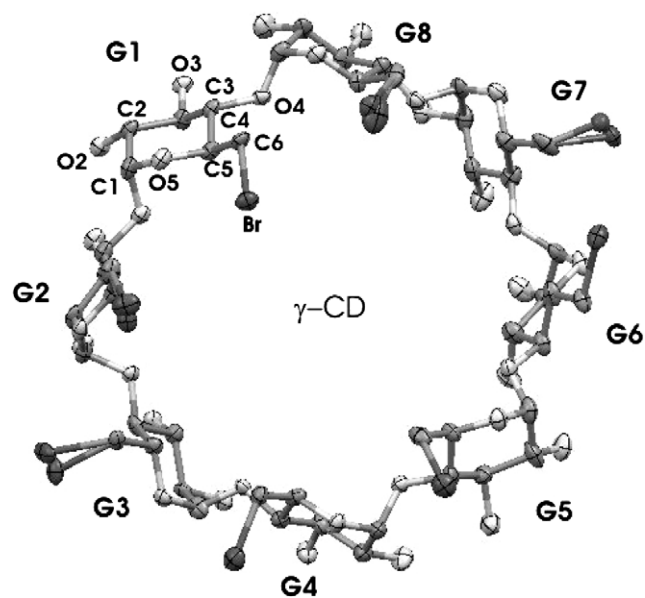


**Figure 1.** ORTEP diagram of  $\gamma$ pBr, molecule B, and numbering scheme.

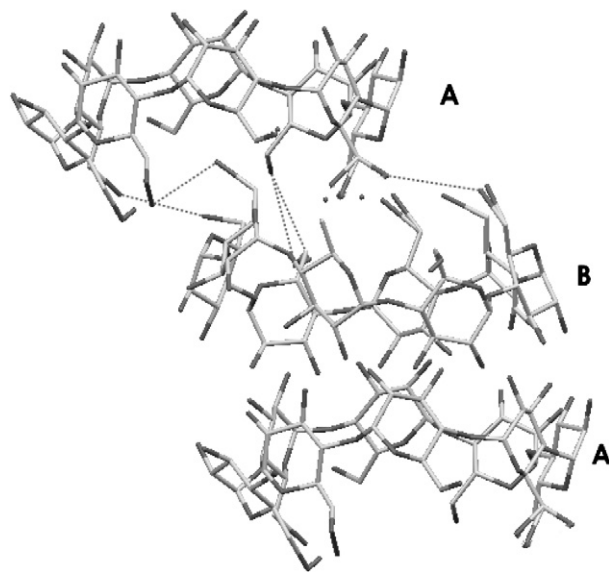


**Figure 2.** The molecules of  $\gamma$ pBr are stacked head-to-head along the *a*-axis, offset from each other. Close contacts among Br atoms are shown.<sup>13</sup>

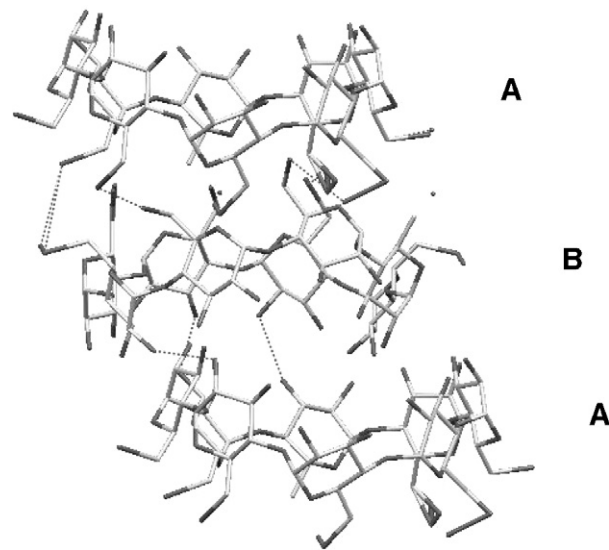


**Figure 3.** The molecular stacking along the *a*-axis at a view rotated by 90° with respect to that of Figure 2. Close contacts among Br atoms and OH atoms are shown.

ecule B, are close to the ideal cyclohexane chair ( $\theta = 0$ ). Table 1 gives selected parameters describing the macrocycle's conformation. The elliptical distortion of the latter is very slight (major and minor O-4*n*...O-4(*n* + 4) distances are 11.26 Å and 10.96 Å for molecule A and 11.53 Å and 11.17 Å for molecule B, respectively). Moreover, the O-4*n*...O-4(*n* + 1) distances and the O-4(*n* - 1)...O-4*n*...O-4(*n* + 1) angles do not differ between the residues and their values are close to those of native  $\gamma$ -CD (4.42–4.60 Å, 131°–137°, respectively).<sup>15</sup> Nevertheless, molecules A and B are quite distorted as seen in Figures 1–3, because of high inward tilt of most

**Table 1.** Conformations of the macrocycle and the glucose units

Glucose unit	$D^i$ (Å)	$\Phi^{ii}$ (deg.)	$D^{iii}$ (Å)	$Q^{iv}$	$\theta^v$ (deg.)	$D_3^{vi}$ (Å)	Tilt angles <sup>vii</sup> (deg.)	O-5 <i>n</i> -C-5 <i>n</i> -C-6 <i>n</i> -Br <sup>viii</sup> (deg.)
G1A	4.32(2)	135.8(3)	0.382(8)	0.5940	2.45	2.82(2)	31.6(5)	−67(2)
G2A	4.41(2)	132.3(3)	0.716(8)	0.5792	3.02	3.05(2)	19.5(9)	−70(2)
G3A	4.42(2)	131.6(3)	−0.531(9)	0.5924	4.48	2.86(2)	18.0(1)	64(2)
G4A	4.22(2)	133.1(4)	−0.646(9)	0.5622	7.93	2.97(2)	34.7(5)	a. 64(2)
								b. 47(2)
G5A	4.51(2)	132.1(4)	0.618(9)	0.5343	4.95	2.72(2)	16.6(4)	a. 73(2)
								b. −13(6)
G6A	4.44(2)	135.7(4)	0.40(1)	0.5893	2.22	2.73(2)	22.9(7)	a. −62(2)
								b. −58(2)
G7A	4.36(2)	131.2(4)	−0.35(1)	0.4893	2.60	2.71(2)	10.0(1)	a. 51(3)
								b. −41(3)
								c. 44(3)
G8A	4.52(2)	132.8(4)	−0.59(1)	0.6083	8.12	2.69(2)	22.0(1)	69(1)
G1B	4.38(2)	130(4)	−0.561(9)	0.5955	2.76	2.90(2)	16.0(1)	a. −63(1)
								b. −76(2)
G2B	4.41(2)	137.1(4)	0.484(9)	0.5534	4.28	2.83(2)	16.0(5)	a. 62(2)
								b. 63(3)
G3B	4.60(2)	133.7(4)	0.595(9)	0.5574	7.64	2.68(2)	32.8(4)	73(1)
G4B	4.29(2)	129.7(4)	−0.33(1)	0.5543	10.34	2.76(3)	25.0(1)	a. 67(2)
								b. 77(2)
G5B	4.32(2)	130.9(4)	−0.93(1)	0.5018	4.09	2.87(2)	28.0(1)	a. −73(3)
								b. −56(3)
G6B	4.50(2)	132.7(4)	0.71(1)	0.6030	5.79	2.80(3)	32.7(5)	60(2)
G7B	4.33(2)	131.4(4)	0.58(1)	0.5196	6.46	2.79(3)	26.0(1)	−63(2)
G8B	4.48(2)	133.7(4)	−0.55(1)	0.5180	4.60	2.67(2)	19.0(1)	−64(2)

<sup>i</sup> O-4*n*...O-4(*n* + 1).<sup>ii</sup> O-4(*n* − 1)...O-4*n*...O-4(*n* + 1) angles.<sup>iii</sup> Deviations (Å) from the least-squares optimum plane of O-4*n* atoms.<sup>iv</sup>  $Q$ : Puckering amplitude, indicates deviation from ideal cyclohexane chair ( $Q = 0.63$  Å).<sup>v</sup>  $\theta$ : Indicates deviation from ideal cyclohexane chair ( $\theta = 0$ ).<sup>vi</sup> Intramolecular H-bonds between O3*n*...O2(*n* − 1).<sup>vii</sup> Tilt angles between the optimum O-4*n* plane and the mean planes through atoms O-4(*n* − 1), C-1*n*, C-4*n*, O-4*n* esds in parentheses.<sup>viii</sup> a,b,c refer to the various orientations of the C-6*n*-Br*n* bond.

glucose units (maximum tilt angle values 34.7° and 32.8° for A and B, respectively) shown in Table 1. Due to this distortion, intramolecular H-bond distances between hydroxyl groups of adjacent residues (O-3*n*...O-2(*n* + 1)) have a wider range (2.67–3.05 Å) than the corresponding distances (2.76–2.91 Å) in native  $\gamma$ -CD. The macrocycle's distortion compares well with permethylated- $\gamma$ -CD<sup>16</sup> and several complexes of permethylated  $\beta$ -cyclodextrin.<sup>17</sup> However, it is not as high as the perbrominated analogue of  $\beta$ pBr, heptakis(6-bromo-6-deoxy-2,3-di-*O*-acetyl)cyclomaltoheptaose, in which the secondary hydroxyl groups are acetylated.<sup>18</sup> Of the other reported CDs persubstituted at the primary side, octakis[6-(2-hydroxyethylthio)-6-deoxy]- $\gamma$ -cyclodextrin<sup>7</sup> with neutral substituents and octakis[6-(4-carboxyphenylthio)-6-deoxy]- $\gamma$ -cyclodextrin<sup>8</sup> with eight negatively charged rigid substituents exhibit lower tilt angles and less distortion of the CD skeleton than  $\gamma$ pBr. Similarly, although in octakis(6-carboxyethylthio)-6-deoxy)- $\gamma$ -cyclodextrin sodium salt<sup>7</sup> two glucose units have higher tilt angles (around 52°) than  $\gamma$ pBr, their primary side tilts outwards and the general distortion is lower.

At the primary side, the C–Br bonds exhibit disorder and a variety of conformations as shown by the O-5*n*–C-5*n*–C-6*n*–Br*n* torsion angles (Table 1): In four

residues of molecule A the Br atoms are disordered: residues G4A, G5A, G6A in two orientations and G7A in three, with major occupancies 90%, 68%, 60% and 60%, respectively. The Br atoms point inward [(+)-gauche with respect to the C-5–O-5 bonds] in three of the latter major conformations, G4A, G5A, G7A, whereas residue, G6A, points outwards [(−)-gauche]. Of the remaining nondisordered Br atoms, two are directed inwards (G3A, G8A) and two outwards (G1A, G2A). Molecule B exhibits four residues, G1B, G2B, G4B and G5B, in which the Br atoms are found in two orientations with major occupancies 90%, 80%, 60% and 89%, respectively. In two of the above major conformations (G2B, G4B) and in two nondisordered (G3B and G6B), the Br atoms point inward.

**Macrocycle packing:** the  $\gamma$ pBr molecules are stacked head-to-head along the *a*-axis forming columns. Despite the molecular and packing differences between  $\gamma$ pBr and  $\beta$ pBr, the two compounds share the common feature that alternate hydrophobic and hydrophilic layers are formed in the crystal. In  $\gamma$ pBr, the parallel arrangement of the columns generates the above layers perpendicular to the stacking axis, in the bc plane (Fig. 4).

Although molecules A and B, being offset from each other by 2.61 Å, do not form proper dimers as in  $\beta$ pBr,

four intermolecular H-bonds between secondary hydroxyl groups (Fig. 3 and Table 2b) hold the two monomers together. On the other hand, at the primary substituted faces, short hydrophobic contacts between Br-atoms contribute further to the cohesion of the columns. Four short intermolecular Br–Br contacts between 3.82 and 3.90 Å are observed (Fig. 2 and Table 2a). In the interacting pairs one Br atom is pointing inwards and the other outwards. Moreover, the Br atoms involved in these short contacts belong to or are located next to the residues that exhibit high tilt angles (in Fig. 2: G4 (34.7°) at the left of top molecule A and G1 (31.60°) and G8 (22°) at the right; G3 (32.8°) and G4 (25°) at the right of molecule B and G6 (32.7°) and G7 (26°) at the left). It is suggested that the strong van der Waals interactions between the Br atoms at the hydrophobic primary sides not only dictate the orientation of the Br atoms but they are also maximised by the macrocycle's distortion. Moreover, they govern the stacking of the  $\gamma$ pBr into alternating hydrophobic and hydrophilic layers in the bc plane.

There are 3.34 water molecules distributed over 8 sites and 4.37 methanol molecules distributed over 8 sites per two monomers in the lattice, of which 6 water and 6 methanol sites are located in the macrocycles' cavities. The numerous intermolecular interactions (Table 2d) between the solvent molecules and monomers A and B, shown schematically in Figure 5, contribute to the stabilisation of the secondary side and the cavity. The difficulty of the two monomers to form proper CD dimers<sup>12</sup> at the secondary side, due to their distorted shape, results in their peculiar association requiring new sources of stabilisation. Thus the energy loss, due to the existence of only four direct H-bonds between the monomers instead of eight in the proper dimer, is compensated by H-bonds of the secondary hydroxyl groups with solvent molecules. Some of these bonds

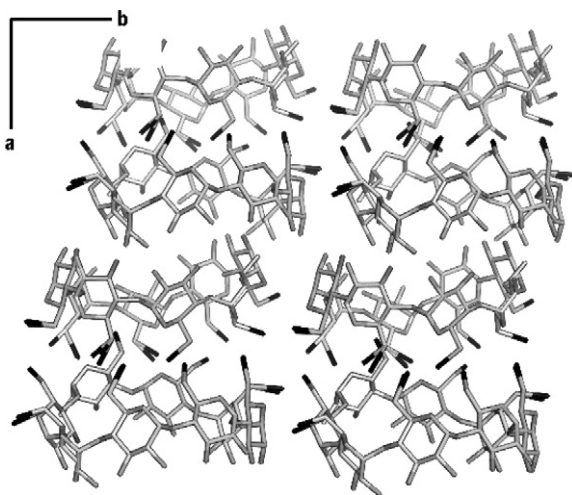


**Figure 4.** Packing of  $\gamma$ pBr molecules along the *a*-axis. The hydrophobic layers perpendicular to *a*-axis are lined by Br atoms (black).<sup>13</sup>

**Table 2.** Intramolecular and intermolecular interactions in the structure of  $\gamma$ pBr

Br...Br	Distance (Å)		
<i>a. Close Br–Br contacts between macrocycles A and B at the primary side</i>			
Br1A...Br1Ba	3.88(1)		
...Br1Bb	3.80(4)		
Br3A...Br8B	3.90(1)		
Br5Aa...Br7B	3.82(1)		
Br7Ab...Br4Ba	3.83(3)		
C–OA...O–CB	Distance (Å)	C–OA...OB (°)	OA...O–CB (°)
<i>b. Direct hydrogen bonds between secondary hydroxyl groups of A and B along the columns</i>			
O38A...O34B	2.92(2)	95(1)	118(2)
O38A...O24B	2.88(3)	147(1)	120(2)
O31A...O33B	2.85(2)	115(1)	98(1)
O23A...O21B	2.87(2)	88(1)	122(1)
<i>c. Direct hydrogen bonds connecting secondary hydroxyl groups of A and B between adjacent columns</i>			
O35A...O22B	2.78(2)	148(1)	110(1)
O26A...O32B	2.72(2)	107(1)	133(1)
O37A...O21B	2.65(2)	128(1)	103(1)
C–OA...OW (°)			
<i>d. H-bonds between secondary hydroxyl groups and solvent molecules.</i>			
C–OA...Osolvent	Distance (Å)	C–OA...OW (°)	
O32A...OW1b	2.94(9)	107(1)	
O25B...OW2a	2.71(5)	110(2)	
O26B...OW3	2.88(3)	123(2)	
O36B...OW3	3.12(3)	115(1)	
O35B...OM3a	2.72(3)	130(2)	
O25B...OM3b	2.58(6)	133(3)	
O36B...OM4	2.67(4)	112(2)	
O33A...OM4	2.98(4)	108(2)	
O22A...OM5	2.84(4)	124(2)	
Osolvent...Osolvent	Distance (Å)		
<i>e. H-bond network among water and methanol molecules entrapped in the cavities of <math>\gamma</math>pBr</i>			
OW1b...OW2a	2.98(10)		
...OW2b	3.12(10)		
...OM6	3.11(10)		
OW2a...OW1c	3.18(6)		
OM2...OM3a	3.11(11)		
OM5...OM6	2.38(6)		
OM6...OW2a	2.77(6)		

indirectly connect hydroxyl groups of the two monomers, as O33A...OM4...O36B. Additional solvent molecules connect hydroxyl groups of  $\gamma$ pBr molecules between columns by H-bonds. Adjacent columns in the lattice are also connected by direct H-bonds between hydroxyl groups (Table 2c). Thus the inside and outside networks of H-bonding strengthen the association of the macrocycles within and between the columns.

Summarising, the  $\gamma$ pBr monomers stack head-to-head forming columns which align in a parallel fashion to form alternating hydrophobic and hydrophilic layers perpendicular to the stacking axis. In contrast to the  $\beta$ pCD analogue,  $\beta$ pBr, which forms dimers of undistorted



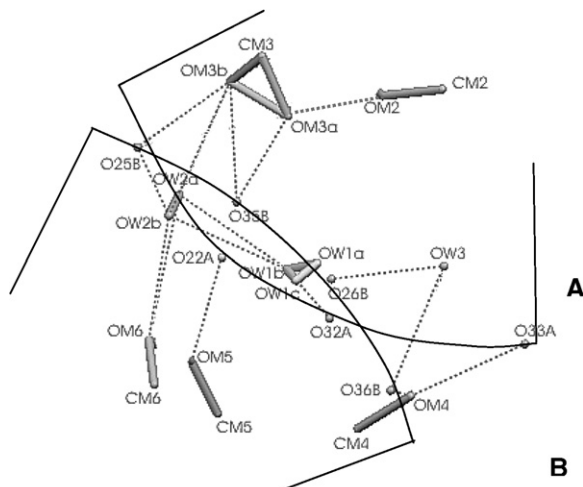


**Figure 5.** Schematic illustration showing the H-bonding network (closest distances) at the secondary side of a  $\gamma$ pBr dimer. OW denotes water oxygen atoms and OM and CM denote methanol atoms.

macrocycles held together by the usual seven H-bonds at the secondary side, the  $\gamma$ pBr monomers associate to form a completely new kind of dimer. The monomers, which are quite distorted, ‘clutch together’ mutually entering into each other both at the primary and the secondary sides. At the primary side they interact by hydrophobic Br–Br interactions and at the secondary side by four direct H-bonds between hydroxyl groups and indirectly through solvent molecules. The short contacts between the Br atoms at the primary side contribute to the macrocycle’s distortion, which is considerable compared to several  $\gamma$ -CDs persubstituted at the primary side with bulkier and in some occasions charged substituents. Water and methanol molecules are entrapped in the macrocycles’ cavities mostly in the area of the secondary hydrophilic side and H-bond to hydroxyl groups of  $\gamma$ pBr. These further strengthen the dimers and contribute to the stabilisation of the cavity and its secondary side periphery.

## 1. Experimental

### 1.1. Synthesis

Octakis(6-bromo-6-deoxy)- $\gamma$ -cyclodextrin ( $\gamma$ pBr) was synthesised as reported previously<sup>19,5</sup> in 86% yield. The compound crystallised as colorless crystals during reaction workup when the methanolic solution containing the product was poured into cold water and allowed to stand.

### 1.2. Crystal structure determination

Low temperature X-ray data were collected at the synchrotron radiation light source at EMBL, DESY,

**Table 3.** Crystal data and structure refinement

Molecular formula	$C_{96}H_{144}Br_{16}O_{64} \cdot 3.34H_2O \cdot 4.37CH_3OH$
Formula weight	3800.87
Temperature	100(2) K
Radiation/wavelength	0.80110 Å
Space group	<i>P</i> 1
<i>a</i> , Å	16.157(17)
<i>b</i> , Å	16.815(22)
<i>c</i> , Å	17.017(28)
$\alpha$ , °	61.53(14)
$\beta$ , °	63.53(8)
$\gamma$ , °	83.96(8)
Volume/ <i>Z</i>	3604(7) Å <sup>3</sup> /1
Density (calculated)	1.751 Mg/m <sup>3</sup>
2 $\theta$ range for data collection	4.65°–27.06°
Index ranges	$0 \leq h \leq 18$ , $-18 \leq k \leq 19$ , $-16 \leq l \leq 19$
Reflections collected/observed	9950/9950
Solution method	Direct methods
Refinement method	Full-matrix least-squares based on $F^2$
Data/restraints/parameters	9950/56/1842
Goodness-of-fit on $F^2$	1.095
Final <i>R</i> indices	$R1 = 0.0945$ , $wR2 = 0.2413$
$[F_o > 4\sigma(F_o)]$	
<i>R</i> indices (all data)	$R1 = 0.0984$ , $wR2 = 0.2466$
Largest diff. peak and hole	0.580 and $-0.499$ e Å <sup>−3</sup>

Hamburg, beamline X13, by the oscillation method using a CCD detector of 165 cm radius. A single crystal, covered with a drop of oil, was mounted on a small loop of hair fiber and was instantly frozen at 100 K. Crystal data and experimental details of X-ray analysis are given in Table 3. The programs DENZO and SCALEPACK<sup>20</sup> were used for data processing and scaling of data, respectively. The unit cell parameters were determined from the post refinement procedure, while their esds from the unit cell parameters of all the frames of data were collected. The structure solution, by direct methods, and the least squares refinement were carried out with the program SHELXL97.<sup>21</sup> All atoms of the macrocycle were treated anisotropically, except for the minor occupancy of Br5B. The refinement of the structure, by  $F^2$  full matrix least squares, converged to  $R1 = 0.0945$ ,  $wR2 = 0.2413$ , goodness of fit = 1.095 for  $F_o > 4\sigma(F_o)$  (Table 3). Hydrogen atoms have been placed in idealised positions in a riding mode ( $U_H = 1.25 U_C$ ). For the disordered 6-CH<sub>2</sub> groups, only H-atoms for the major orientations were placed.

### Supplementary data

Complete crystallographic data for the structural analysis have been deposited with the Cambridge Crystallographic Data Centre, CCDC No. 635578. Copies of this information may be obtained free of charge from the Director, Cambridge Crystallographic Data Centre,

12 Union Road, Cambridge, CB2 1EZ, UK. (fax: +44-1223-336033, e-mail: deposit@ccdc.cam.ac.uk or via: [www.ccdc.cam.ac.uk](http://www.ccdc.cam.ac.uk)).

### Acknowledgements

NCSR 'Demokritos' (for scholarships to A.P, P.G. and N.M.) is gratefully acknowledged. The financial support from General Secretariat of R&D of Greece (program PRAXE), the support of Empirikion Foundation and Marie Curie training site programme (HPMT-CT-2000-00174) are also kindly acknowledged.

### References

- Khan, A. R.; Forgo, P.; Stine, K. J.; D'Souza, V. T. *Chem. Rev.* **1998**, 98, 1977–1996.
- Gadelle, A.; Defaye, J. *Angew. Chem., Int. Ed. Engl.* **1991**, 30, 78–80.
- Baer, H. H.; Berenguel, A. V.; Shu, Y. Y.; Defaye, J.; Gadelle, A.; Gonzalez, F. S. *Carbohydr. Res.* **1992**, 228, 307–314.
- Ling, C.-C.; Darcy, R. *J. Chem. Soc., Chem. Commun.* **1993**, 438–440.
- Vizitiu, D.; Walkinshaw, C. S.; Gorin, B. I.; Thatcher, G. R. J. *J. Org. Chem.* **1997**, 62, 8760–8766.
- Nicolis, I.; Coleman, A. W.; Charpin, P.; Villain, F.; Zhang, P.; Ling, C. C.; de Rango, C. *J. Am. Chem. Soc.* **1993**, 115, 11596–11597.
- Adam, J. M.; Bennett, D. J.; Bom, A.; Clark, J. K.; Feilden, H.; Hutchinson, E. J.; Palin, R.; Prosser, A.; Rees, D. C.; Rosair, G. M.; Stevenson, D.; Tarver, G. J.; Zhang, M.-Q. *J. Med. Chem.* **2002**, 45, 1806–1816.
- Cooper, A.; Nutley, M.; MacLean, E. J.; Cameron, K.; Fielding, L.; Mestres, J.; Palin, R. *Org. Biomol. Chem.* **2005**, 3, 1863–1871.
- Bom, A.; Bradley, M.; Cameron, K.; Clark, J. K.; van Egmond, J.; Feilden, H.; MacLean, E. J.; Muir, A. W.; Palin, R.; Rees, D. C.; Zhang, M.-Q. *Angew. Chem., Int. Ed.* **2002**, 41, 265–270.
- Johnson, C. K. ORTEP, ORNL-5138; Oak Ridge National Laboratory: Tennessee, USA, 1973.
- Mentzafos, D.; Mavridis, I. M.; Le Bas, G.; Tsoucaris, G. *Acta Crystallogr. B* **1991**, 47, 746–757.
- Makedonopoulou, S.; Mavridis, I. M. *Acta Crystallogr. B* **2000**, 56, 322–331.
- Bruno, I. J.; Cole, J. C.; Edgington, P. R.; Kessler, M. K.; Macrae, C. F.; McCabe, P.; Pearson, J.; Taylor, R. Graphics program 'MERCURY'. *Acta Crystallogr. B* **2002**, 58, 389–397.
- Cremer, D.; Pople, J. A. *J. Am. Chem. Soc.* **1975**, 97, 1354–1358.
- Harata, K. *Bull. Chem. Soc. Jpn.* **1987**, 60, 2763–2767.
- Aree, T.; Hoier, H.; Schultz, B.; Reck, G.; Saenger, W. *Carbohydr. Res.* **2000**, 328, 399–407.
- Rontoyianni, A.; Mavridis, I. M.; Israel, R.; Beurskens, G. *J. Incl. Phenom. Mol. Recognit. Chem.* **1998**, 32, 415–428.
- Giasas, P.; Eliadou, K.; Plyta, Z. F.; Yannakopoulou, K.; Mavridis, I. M. *Carbohydr. Res.* **2004**, 339, 1189–1194.
- Mourtzis, N.; Eliadou, K.; Aggelidou, C.; Sophianopoulou, V.; Mavridis, I. M.; Yannakopoulou, K. *Org. Biomol. Chem.* **2007**, 5, 125–131.
- Otwinowski, Z.; Minor, W. Processing of X-ray Diffraction Data Collected in Oscillation Mode. In *Macromolecular crystallography, Part A*; Carter, C. W., Jr, Sweet, R. M., Eds.; Methods in Enzymology; Academic Press: New York, 1997; Vol. 276, pp 307–326.
- Sheldrick, G. M. SHELXL97; University of Goettingen: Goettingen, Germany, 1997.